Maldistribution in Fluidized Beds

Rex B. Thorpe*

School of Engineering (D2), University of Surrey, Guildford GU2 7XH, U.K.

John F. Davidson, Michael Pollitt, and Jason Smith

University of Cambridge, Department of Chemical Engineering, Pembroke Street, Cambridge CB2 3RA, U.K.

Experiments on maldistribution were performed using a 289 mm diameter air−sand fluidized bed with a multiorifice distributor. The minimum superficial gas velocity (U_m) required to eliminate maldistribution was measured; the results were combined with those in the literature and used to evaluate the following rules for maldistribution: (1) the pressure drop ratio method, that is, a specified ratio of distributor pressure drop to bed pressure drop, R, as recommended by Perry et al.,[1] (2) the theory of Fakhimi and Harrison,[2] based on a pressure balance for the gas passing through active and inactive gas injection points at the distributor, and (3) the theory of Yue and Kolaczkowski,[3] a modification of Fakhimi and Harrison's theory.[2] The data cover a variety of bed sizes and shapes including the industrially sized beds of Whitehead and Dent,[4] who used tuyere distributors. The best agreement was found with the theory of Fakhimi and Harrison,[2] which gives a simple formula for predicting U_m if combined with reliable predictions[2,5] for the height of the entry zone, h. The average error in predicting U_m this way was 18%, and the largest error was a factor of 2. The traditional method,[1] using a specified R, shows a largest error of a factor of 6 in U_m if the best value of R is used.

1. Introduction

Gas−solid fluidized beds find a variety of applications in industry: catalytic reactors, combustion chambers, and dryers. In a fluidized bed, gas is passed through a bed of solid particles. When the flow is such that the pressure drop across the bed is sufficient to support the weight of the particles, the bed is said to be incipiently fluidized and the solid particles move about, resembling a liquid. Gas flow in excess of that required for incipient fluidization passes through the bed as bubbles. When the gas velocity exceeds the value required for incipient fluidization, U_{mf}, the gas bubbles are observed not to be in some parts of the bed (dead zones), which usually occur near to the distributor. The bubbling areas and the dead zones often move with time. In this state, the bed is said to be maldistributed (see Figure 1). However, if the superficial gas velocity is increased above a certain value, U_m, the bubbles become uniformly distributed and the bed is termed evenly fluidized.

Maldistribution is industrially undesirable: for dryers, because the dead zones may dry very slowly, and for reactors, because there will be bypassing of reactants and the temperature in the bed will be uneven. The aim of this paper is to predict the boundary between maldistribution and even fluidization, that is, the value of U_m, and thereby enable designers to avoid maldistribution with minimal energy consumption due to the distributor plate.

1.1. Background. Over the past 35 years a number of authors have specified that the ratio R of distributor pressure drop, ΔP_d, to bed pressure drop, ΔP_b, should be greater than a certain critical value to ensure even fluidization. Perry et al.[1] specify R of $^1/_3$. However, there is no consensus in the literature (see Table 1), with recommended critical values of R in the range 0.02 to 1 being recommended.[6]

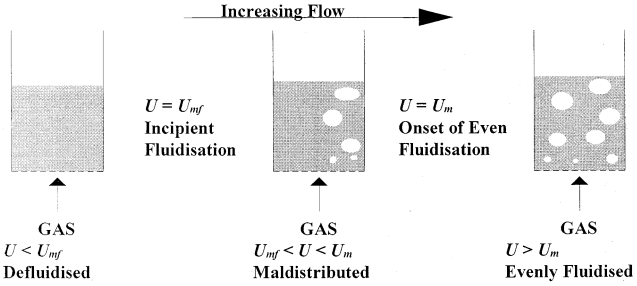

Figure 1. Diagram showing a maldistributed bed and an evenly fluidized bed.

Table 1. Examples of Critical Values of *R* for Even Fluidization

authors	min value of R	notes
Zenz and Othmer[7]	0.4	
Agarwal et al.[8]	0.1	$\Delta P_{d,min} > 3400$ Pa
Hiby[9]	0.15	$U_m/U_{mf} < 2$
	0.015	$2 < U_m/U_{mf}$
Avery and Tracy[10]	1	
Perry et al.[1]	0.3	
Thorpe et al.[11]	0.5−1	$U_m/U_{mf} \approx 1$
	0.05−0.1	$2 \ll U_m/U_{mf}$

However, Thorpe et al.[11] have cast doubt on this method of predicting maldistribution and therefore its utility for distributor design. It can be tested easily against experimental data for critical values of R taken from the literature and from the experiments reported in this paper (see Table 2 for details). This data set represents a wide variety of sizes and shapes of rig with both multiorifice and tuyere distributors.

* Corresponding author. E-mail: ces2rt@surrey.ac.uk. Fax: +44-1483-686581. Telephone: +44-1483-689270.

10.1021/ie0203173 CCC: $22.00
Published on Web 10/12/2002

Table 2. Sources of Experimental U_m Values

Whitehead and Dent[4]	3D beds (up to 1200 mm × 1200 mm) with tuyere distributors
Dusad[12] and Downing[13]	3D bed (200 mm × 100 mm) with multiorifice distributor
Yue and Kolaczkowski[3]	2D[a] bed (815 mm × 14 mm) with multiorifice distributor[b]
this project	3D bed (289 mm diameter) with multiorifice distributor

[a] A two-dimensional (2D) bed is one that is very thin in one horizontal direction. [b] The data of Yue and Kolaczkowski are incomplete for the purpose to which they are put in this paper, and therefore certain parameters have been estimated as described in Appendix 1.

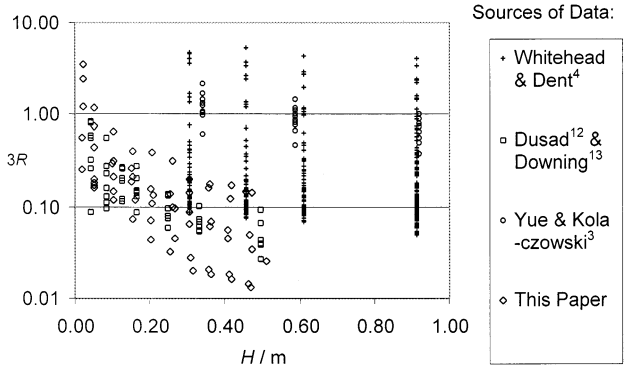

Figure 2. Graph to evaluate the effectiveness of the method of Perry et al.,[1] using $3R = 1$, to predict maldistribution.

Figure 2 shows experimental values of R for the onset of maldistribution divided by the prediction of Perry et al.[1] ($R = {}^1/_3$) plotted against the height of the fluidized bed, H, although it appears to be a variable of little consequence. It can be seen that the prediction using $R = {}^1/_3$ is often very conservative but may be inadequate to prevent maldistribution: a significant number of data points lie above the line $3R = 1$. Overall, R varies experimentally by a factor of around a thousand, so no single value of R can match experimental data. If a very large value of R is chosen for design, it will, in many cases, be very wasteful in terms of the energy required to pump the fluidizing gas through the distributor plate. If a lower value is chosen, there is a risk of maldistribution.

Two review articles[6,14] give correlations for R as a function of the bed aspect ratio: bed diameter (D)/bed height (H). Qureshi and Creasy[14] cite a variety of experimental data, mostly for systems with even fluidization, rather than at the limit of maldistribution. We examine the role of bed height H in section 3.5 below and find it a minor effect, as suggested by Figure 2. It is a main conclusion of this paper to reject the use of R as a parameter for distributor design.

Thorpe et al.[11] also demonstrated, using most of the data set outlined above, that the equation recommended by Sathiymoorthy and Shridar Rao,[15] which correctly predicts that R decreases with increase of U_m/U_{mf}, is, nonetheless, too conservative by a significant factor, especially at low values of U_m/U_{mf}.

1.2. Fakhimi and Harrison.[2] Their theory, for a perforated plate distributor, is discussed in detail by Davidson et al.[16] In outline, the model rests on the following assumptions (see Figure 3): (a) at incipient fluidization, none of the orifices is jetting and each has a flow q_{mf}; (b) flow in excess of the flow for incipient fluidization is not shared evenly between the orifices but instead causes some of them to start jetting, which requires a flow which is greater by the finite quantum δq; and (c) the sum of the orifice pressure drop and the pressure drop across the entry zone of the bed is the same for all orifices (that is, there is a uniform pressure

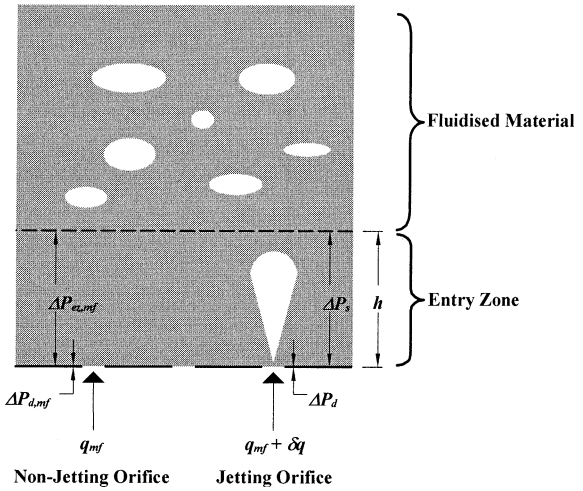

Figure 3. Theoretical model of Fakhimi and Harrison.[2]

at the top of the entry zone). Thus, referring to Figure 3, we equate pressure drops (i) and (ii), which are (i) across the nonjetting orifices and the entry zone and (ii) across the jetting orifices and the entry zone, giving

$$\Delta P_{ez,mf} + \Delta P_{d,mf} = \Delta P_d + \Delta P_s \qquad (1)$$

Here, $\Delta P_{ez,mf} = \rho_s(1 - \epsilon_{mf})gh$ is due to the weight per unit area of the incipiently fluidized entry zone, $\Delta P_s = (2/\pi)\rho_s(1 - \epsilon_{mf})gh$ is the pressure drop across a jet,[17] ρ_s is the solid density of the particles, and ϵ_{mf} is the voidage fraction at incipient fluidization.

The distributor pressure drop is found from orifice theory:

$$\Delta P_d = \frac{\rho_g q^2}{2(c_d a_o)^2} = K_p \rho_g U^2 \qquad (2)$$

Thus, the pressure balance, eq 1, can be rearranged to give an expression for the fraction of the orifices that are jetting as a function of flow. Davidson et al.[16] suggested that the bed is evenly fluidized when all orifices are jetting, which defines U_m. This implies that (the pressure drop across the entry zone at velocity U_{mf} + the pressure drop across the entry zone at velocity U_{mf}) = (the pressure drop across the entry zone at velocity U_m + the pressure drop across the entry zone at velocity U_m). Thus, $\rho_s(1 - \epsilon_{mf})gh + K_p\rho_g U_{mf}^2 = (2/\pi)\rho_s(1 - \epsilon_{mf})gh + K_p\rho_g U_m^2$, which, after rearrangement, leads directly to

$$\frac{U_m}{U_{mf}} = \left(1 + \frac{\rho_s g\left(\left[\frac{h}{s}\right]s\right)\left(1 - \frac{2}{\pi}\right)(1 - \epsilon_{mf})}{\rho_g K_p U_{mf}^2}\right)^{0.5} \qquad (3)$$

The height of the entry zone (h) is most conveniently obtained as a multiple of the orifice spacing (s) by correlations that depend on the type of bed (s is always

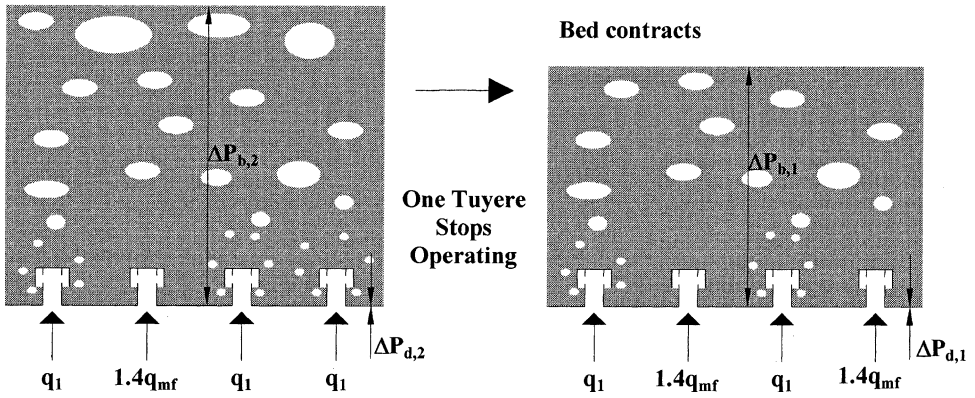

Figure 4. Whitehead and Dent[4] theoretical model.

known). The following proposals are to be found in the literature:

2D beds (multiorifice distributors)[2]

$$h/s = 3.8 \tag{4}$$

3D beds (multiorifice distributors)[5]

$$h/s = 2 \tag{5}$$

3D beds with horizontal injection (tuyere distributors)[18,19]

$$h/s' = 0.5 \tag{6}$$

Here s' is the modified tuyere spacing, that is, s, the center to center distance, minus the tuyere diameter.

The height of the entry zone is further considered in section 4. Equation 3 is compared to the experimental data set in section 4.

1.3. Whitehead and Dent.[4] Along with their experimental data, Whitehead and Dent[4] present a semitheoretical analysis that shows similarities to the above; the basis of the analysis is shown in Figure 4.

They consider the tuyeres to be either nonoperating, each with a flow of $1.4q_{mf}$, obtained from measurements on individual tuyeres, or operating, with the remaining flow equally divided between them and with a flow to each tuyere, q_1, greater than $1.4q_{mf}$.

They consider the case when one extra tuyere becomes nonoperating and the excess gas is redistributed among the remaining operating tuyeres. This causes an increase in the value of q_1 and therefore an increase in ΔP_d. They assume it to cause a fractional contraction in the bed, presumably due to less bubble volume. This is assumed to cause a reduction in ΔP_b, as a constant pressure drop per unit height is assumed. This last assumption is contrary to the normal assumption of aggregative fluidization, which assumes that ΔP_b is constant and equal to that value required to support the weight of the bed. Although other work (section 4) has shown that ΔP_b is a little less than the pressure drop required to support the weight of the bed, $(\rho_s(1 - \epsilon_{mf})gH)$, this is due to effects in the entry zone. The pressure gradient with respect to height is certainly not constant when the bed contracts. We therefore reject the detail of the theoretical aspect of the work of Whitehead and Dent.[4] However, the general idea of a pressure balance across the entry region of the fluidized bed shows some similarity to the analysis of Fakhimi and Harrison[2] above. There is no fundamental difference between a multiorifice distributor and one made of tyueres in this respect. Therefore, because the analysis of Whitehead and Dent[4] has similarities to that of Fakhimi and Harrison[2] and because the final equation of Whitehead and Dent[4] is semiempirical and fits their own data well, we will continue to discuss it's development.

The fractional contraction in the bed is not quantified by Whitehead and Dent;[4] it is absorbed into an empirical constant. The resulting formula for U_m, the superficial velocity to make all tuyeres operate (in the units used by Whitehead and Dent[4]), is

$$\frac{U_m}{U_{mf}} = 0.7 + \left(0.49 + \frac{kN^{0.22}K_D{}^2\rho_s D_s}{U_{mf}{}^2}\right)^{0.5} \tag{7}$$

Here D_s is the defluidized bed depth (ft) and K_D is the *grate flow factor* (60 ft/(s (in wg)$^{0.5}$)). Here "in wg" means pressure in inches water gauge. The other quantities in eq 7 are also in Imperial units. Imperial units are known as English units in the USA.

Equation 7 can be converted to the following formula in SI units:

$$\frac{U_m}{U_{mf}} = 0.7 + \left(0.49 + \frac{k'N^{0.22}\rho_s H}{\rho_g K_p U_{mf}{}^2}\right)^{0.5} \tag{8}$$

Whitehead and Dent[4] claim that eq 7, with $k = 3.23 \times 10^{-7}$ (in wg ft^2/3600 lb), that is, $k' = 0.060$ (m/s^2) in eq 8, gives a correlation of their experimental data with an "average" error of 10%. The factors of 0.7 and 0.49 arise from the assumption that the flow through a nonoperating tuyere is $1.4q_{mf}$. This has not been used in any other theories, probably because, for multiorifice distributors, U_m is sometimes less than $1.4U_{mf}$ (so the flow through a nonoperating orifice cannot possibly be $1.4q_{mf}$).

For the majority of Whitehead and Dent's data, $U_m > 1.4U_{mf}$. Furthermore, the empirical constants were determined for a data set only for tyuere distributors. Nonetheless, there are some striking identities between eqs 8 and 3. They are, the index of 0.5, the appearance of ρ_s in the numerator, and the appearance of ρ_g, K_p, and U_{mf} in the denominator of the fraction. However, the following differences should also be noted. (a) The leading constants, 1 and $(0.7 + 0.49^{0.5}) = 1.4$, respectively, are not quite the same. (b) Equation 3 does not depend on the height of the material in the bed, H. (c) Equation 8 lacks g, which explains the dimensions of the constant k'. (d) The variation with the number of orifices is different: eq 8 has the fraction varying as

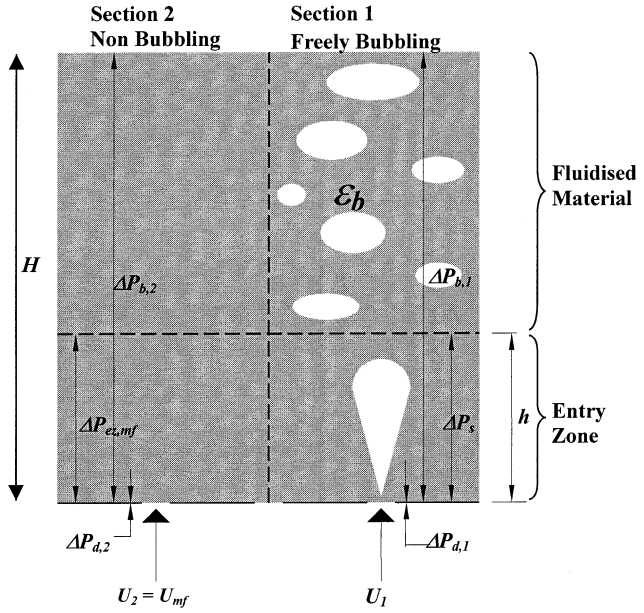

Figure 5. Yue and Kolaczkowski[3] theoretical model.

$N^{0.22}$ whereas eq 3 has a variation with s, which in turn is proportional to $N^{-0.5}$.

With respect to difference b, Whitehead and Dent[4] report no effect of H above 3 ft. In respect to difference d, the reason Whitehead and Dent[4] included the term $N^{0.22}$ is suspect. It is an empirical addition that has little justification in the data they present. Therefore, although there is similarity between eq 3, Fakhimi and Harrison,[2] and eq 7, Whitehead and Dent,[4] and although the later gives roughly the right trend of R with U_m/U_{mf}, it is unlikely to enjoy universal application.

1.4. Yue and Kolaczkowski.[3] This theory builds on the ideas of Fakhimi and Harrison,[2] and its basis is shown in Figure 5. Again, the orifices are considered either to be (i) incipiently fluidized, that is, neither jetting nor bubbling (section 2 of the bed), or (ii) to be jetting and bubbling (section 1 of the bed). Flow in excess of incipient fluidization is shared among the jetting orifices only, so for jetting orifices $q > q_{mf}$ and for nonjetting orifices $q = q_{mf}$. The flows through the orifices are converted to superficial velocities, giving the difference in pressure drops for the distributor as

$$\Delta P_{d,1} - \Delta P_{d,2} = \frac{{}^1/_2\rho_f A^2(U_1{}^2 - U_{mf}{}^2)}{c_d{}^2 N^2 a_o{}^2} = \Delta P_{d,mf}\left(\frac{U_1{}^2}{U_{mf}{}^2} - 1\right) \quad (9)$$

where the superficial velocity in section 1 of the bed $U_1 = (N/n)(U - U_{mf}) + U_{mf}$.

The bed side of the pressure balance has two terms. Somewhat simplistically, the bubbles are assumed to rise only above the active orifices (section 1 of the bed); hence, this part of the bed has a lower bulk density, described by the bubble volume fraction, ϵ_b. Thus, there is the following difference in pressure drop between the two sections to the top of the entry zone: $\epsilon_b\rho_s g(1 - \epsilon_{mf})$-$(H - h)$. In our experiments, described below, when the bed was maldistributed, bubbles burst on only part of the surface of the bed, so this idea has intuitive attraction. However, we do not know the paths taken by the bubbles from the distributor by visual observation, so the bed may not actually have well-defined sections.

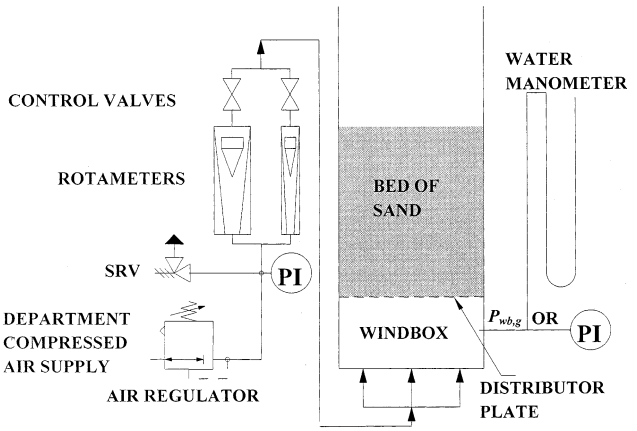

Figure 6. Experimental apparatus.

Yue and Kolaczkowski's paper does not have the term in h shown above, and they also simplify the expression for pressure difference by arguing that, because $\epsilon_b \ll 1$, H can be approximated by H_{mf} to give the pressure difference between the two sections above the top of the entry zone:

$$\epsilon_b\rho_s g(1 - \epsilon_{mf})H_{mf}\ [= \epsilon_b\Delta P_{b,mf}] \quad (10)$$

The pressure drop difference due to the jets is the same as that in the analysis of Fakhimi and Harrison[2]:

$$\Delta P_{ez,mf} - \Delta P_s = \left(1 - \frac{2}{\pi}\right)\rho_s g(1 - \epsilon_{mf})h = \left(1 - \frac{2}{\pi}\right)\frac{h}{H_{mf}}\Delta P_{b,mf} \quad (11)$$

The pressure drop differences from the erroneous version of eq 10 and from eq 11 were added by Yue and Kolaczkowski to give the overall bed pressure drop difference:

$$\Delta P_{b,2} - \Delta P_{b,1} = \rho_s g(1 - \epsilon_{mf})(\epsilon_b H_{mf} + (1 - 2/\pi)h) \quad (12)$$

We now equate the distributor and bed pressure drop differences, eqs 9 and 12: using the second part of eq 9, with $\Delta P_{d,mf} = K_p\rho_g U_{mf}{}^2$ from eq 2, gives the following expression for the fraction of orifices which are operating.

$$\frac{n}{N} = \frac{U/U_{mf} - 1}{\left(\dfrac{\rho_s g(1 - \epsilon_{mf})(\epsilon_b H_{mf} + (1 - 2/\pi)h)}{\rho_g K_p U_{mf}{}^2} + 1\right)^{0.5} - 1} \quad (13)$$

Again, assuming that the bed is evenly distributed when all the orifices are operating ($n/N = 1$), Yue and Kolaczkowski[3] derive an expression for U_m which can be rewritten, directly from eq 13, as

$$\frac{U_m}{U_{mf}} = \left(1 + \frac{\rho_s g(1 - \epsilon_{mf})(\epsilon_b H_{mf} + (1 - 2/\pi)h)}{\rho_g K_p U_{mf}{}^2}\right)^{0.5} \quad (14)$$

This can be compared to eq 3:[2] eqs 3 and 14 are the same excepting the extra $\epsilon_b H_{mf}$ term in eq 14 that comes

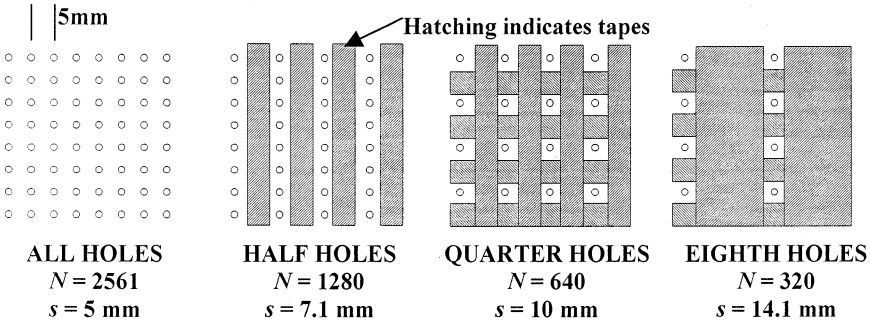

Figure 7. Diagram showing how the orifices were taped up.

Table 3. Distributor Plates

distributor	holes	pitch	sand size range
A	i.d. 1.50 ± 0.05 mm	5 mm, square	P: 600−850 μm
B	i.d. 0.92 ± 0.02 mm	5 mm, square	Q: 200−400 μm

from including a pressure drop difference above the entry zone.

Yue and Kolaczkowski[3] claim that eq 14 gives a better agreement with experimental data than the theory of Fakhimi and Harrison[2] (eq 3). Equation 14 is compared with experimental results in section 5.2.

2. Experimental Section

Experiments were conducted in a 289 mm diameter, 1.5 m high fluidized bed with an air supply and the instrumentation shown in Figure 6. Two distributor plates were used. Distributor A was manufactured by punching holes in a flat plate of mild steel. This left burrs at the edges of the holes, painstakingly removed by drilling. Distributor B was manufactured from a 2 mm thick stainless steel plate by laser drilling, which left no burrs. In both cases, the holes in the plates were examined for the quality of the finish and the variation on hole size. Each plate had the same number and arrangement of holes. Each plate had a corresponding size of sand, as shown in Table 3: the ratio (sand particle size)/(hole diameter) was as small as possible, consistent with the requirement that few particles should fall through the holes during filling and operation. Thus, two sizes of sand were used, because sand Q dropped through the holes in distributor A and also because the second size of sand allowed us to vary another experimental parameter, namely the particle diameter. The sand was sourced from Leighton Buzzard and dried and sieved by David Ball Limited, Bar Hill, Cambridge. The sand was angular ("sharp") and of solid density 2600 kg m^{-3}. Sand P is class D according to the classification of Geldart,[20] and sand Q is in class B.

The pressure drop across the distributor plate, with no sand in the bed, was measured as a function of flow, to find the distributor characteristic, K_p, defined by eq 2 above.

A weighed mass of sand (m) was added to the bed. This was then vigorously fluidized to remove any consolidation. The wind box pressure was measured as a function of gas flow, with the flow being both increased and decreased.

Farthing[21] and Ferdinando[22] concluded that the best way to judge the transition between maldistribution and even fluidization is to observe the bed visually. Whitehead et al.[23] suggest that maldistribution can occur due to bubble coalescence, despite uniform fluidization at the distributor. Therefore, visual observation of the top of the bed was used to judge whether any part of the bed was maldistributed. In this way, the minimum velocity for uniform fluidization, U_m, was measured; U_m was always determined by decreasing the flow from a value sufficient to give a good distribution.

The experiment was repeated with various values of sand mass, m, in the bed (up to 49 kg). Also, the pressure drop characteristic of the distributor plate was altered systematically by covering up holes on the underside of the disributor with masking tape, as shown in Figure 7, and the experiments described above were repeated.

When half or an eighth of the orifices were open, the orifice spacing (s) depends on direction. For theoretical work, s was calculated from s^2N = constant, as suggested by a reviewer. See also Table 7 below.

3. Results and Discussion

The results are given in Table 4.

3.1. Distributor Characteristics. The dimensionless distributor characteristic, K_p, is defined in eq 2. Note that as K_p was measured without the bed of sand, the distributor pressure drop (ΔP_d) = wind box gauge pressure ($P_{wb,g}$). K_p was thus obtained by a least-squares fit of ΔP_d against U^2, with the fit forced through the origin.

The theoretical distributor characteristic was calculated from eq 2 with $Nq = UA$, giving

$$K_p = \frac{1}{2}\left(\frac{A}{Nc_d a_o}\right)^2 \tag{15}$$

Discharge coefficients (c_d) were predicted using[14]

$$c_d = 0.82\left(\frac{d_o}{t}\right)^{-0.13} \tag{16}$$

Equation 16 predicts c_d of 0.85 for distributor A and 0.91 for distributor B, considerably higher than the usual value of 0.64 for sharp edged orifice plates. Table 5 compares experimental and theoretical K_p values (multiple values indicate repeated experiments).

With all of the orifices uncovered, the agreement between experiment and theory is good, hence verifying the correlation[14] for c_d, eq 16. When orifices are taped up, the experimental K_p is below the theoretical value, which corresponds to a lower ΔP_d, consistent with a small amount of air leaking past the tape. This is not thought to affect the validity of the experimental measurements.[26] The experimental value of K_p has been used for the theoretical predictions of maldistribution given in section 5.

Table 4. Experimental Results[a]

distributor A (d_o = 1.5 mm)				distributor B (d_o = 0.92 mm)			
m/kg	H/m	U_{mf}/m·s^{-1}	U_m/m·s^{-1}	m/kg	H/m	U_{mf}/m·s^{-1}	U_m/m·s^{-1}
All Holes Open. K_p = 150				All Holes Open. K_p = 897			
5	0.052	0.320	0.494	2	0.02	0.123	0.151
5	0.052	0.317	0.477	5	0.05	0.109	0.204
10	0.102	0.366	0.576	10	0.102	0.103	0.260
15	0.153	0.399	0.553	15	0.16	0.102	0.292
20	0.204	0.366	0.494	20	0.204	0.103	0.256
25	0.254	0.378	0.472	25	0.267	0.074	0.236
30	0.309	0.361	0.485	30	0.316	0.117	0.168
35	0.356	0.398	0.448	35	0.363	0.114	0.173
40	0.41	0.392	0.447	40	0.417	0.120	0.175
45	0.462		0.420	45	0.47	0.128	0.166
				49	0.511	0.118	0.171
Half Holes Open. K_p = 553				Half Holes Open. K_p = 3122			
2	0.021		0.427	2	0.02		0.121
5	0.051	0.373	0.408	5	0.05	0.107	0.114
10	0.104	0.345	0.491	10	0.102	0.107	0.167
15	0.154	0.397	0.487	15	0.152	0.117	0.193
20	0.208	0.394	0.455	20	0.206	0.107	0.171
25	0.261	0.395	0.437	25	0.267	0.107	0.182
30	0.307	0.399	0.446	30	0.305	0.106	0.162
35	0.364	0.363	0.429	35	0.359	0.107	0.169
40	0.409	0.352	0.407	40	0.407	0.109	0.154
45	0.466		0.410	45	0.472	0.113	0.145
				49	0.511	0.112	0.130
Quarter Holes Open. K_p = 1611				Quarter Holes Open. K_p = 8873			
2	0.021		0.428	2	0.021	0.115	0.152
5	0.051		0.387	5	0.05	0.109	0.131
10	0.102	0.370	0.409	10	0.101	0.107	0.116
15	0.154	0.384	0.394	15	0.152	0.108	0.135
20	0.207	0.372	0.452	20	0.202	0.110	0.121
25	0.259	0.390	0.455	25	0.253	0.115	0.128
30	0.307	0.365	0.393	30	0.305	0.120	0.140
35	0.361	0.379	0.400	35	0.357	0.127	0.163
40	0.417	0.407	0.426	40	0.415	0.141	0.153
45	0.456		0.415	45	0.472	0.155	0.176
				49	0.511	0.155	0.161

[a] See section 2 for experimental details. All data for U_m refer to decreasing flow.

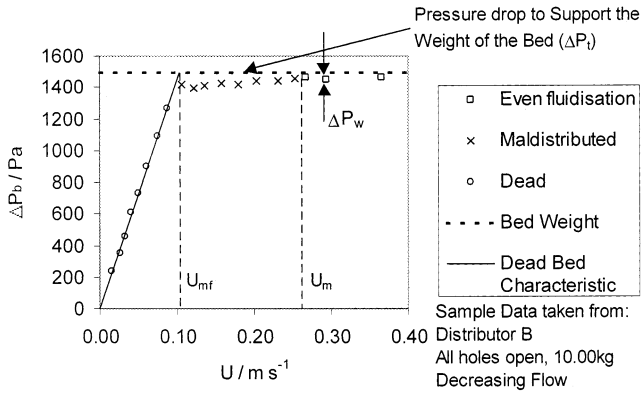

Figure 8. Typical graph of bed pressure drop, as a function of flow, showing how U_{mf} and U_m were found.

Table 5. Dimensionless Distributor Characteristics (K_p)

distributor	fraction of holes active	exp K_p	theor K_p (eqs 15 & 1)
A	all	150 ± 1, 144 ± 1	149
A	half	553 ± 3	596
A	quarter	1611 ± 7, 1768 ± 10	2384
A	eighth	7430 ± 32, 6064 ± 25	9535
B	all	897 ± 10	897
B	half	3122 ± 30	3591
B	quarter	8873 ± 89	14363

3.2. Superficial Velocity for Incipient Fluidization (U_{mf}). Figure 8 shows a typical plot of bed pressure drop as a function of superficial gas velocity. U_{mf} was obtained from the intersection of the line for pressure drop across the defluidized (dead) bed and the horizontal dashed line representing the theoretical pressure drop to support the weight of the bed (ΔP_t). Note that sand P has a particle Reynolds number of ~60, so inertial effects are significant and therefore the well-known Ergun equation was used to generate the defluidized bed line, which in turn was not always quite straight.

Table 6. Average U_{mf} for Each Size of Sand

sand	avg exp U_{mf}/m·s^{-1}	theor U_{mf}/m·s^{-1}
P (600−850 μm)	0.374 ± 0.005	0.48 ± 0.10
Q (200−400 μm)	0.113 ± 0.003	0.11 ± 0.06

Table 6 gives the average experimental U_{mf} values. Values for each experiment are in Table 4. The experimental U_{mf} can be compared to theoretical values calculated using the Ergun equation, with ϵ_{mf} = 0.43 (estimated from bed height measurements). The particle diameter (d_p) was taken as the average of the maximum and minimum sand sizes.

3.3. Superficial Velocity at the Onset of Even Fluidization (U_m). Graphs such as Figure 8 were also used to evaluate U_m. U_m was taken as the average of the last maldistributed reading of U and the first evenly fluidized one. U_m values from each experiment are given in Table 4. A typical estimate of uncertainty in an individual measurement of U_m is ±4%, which is smaller than the scatter of the data in Figures 17 and 18.

3.4. Comparison between Experiments with Increasing and Decreasing Flow. It is generally ac-

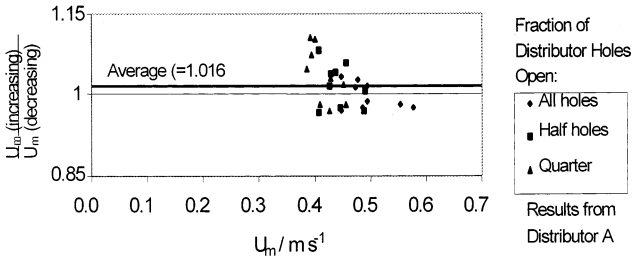

Figure 9. Graph to compare U_m on increasing and decreasing flow for sand P.

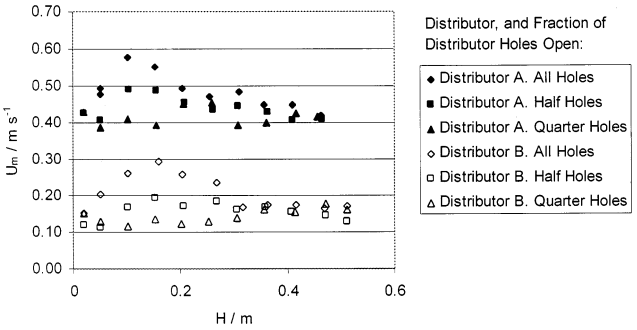

Figure 10. Graph to show the effect of bed height on U_m. See Table 3 and Figure 7 for distributor details.

cepted that there is some hysteresis in fluidized systems:[2] more flow is required to get even fluidization than is required to sustain it. This can be tested by comparing U_m for increasing and decreasing flow situations, as shown in Figure 9 for sand P.

On average, U_m was slightly higher when the flow was being increased. The magnitude of the difference is much less than the scatter in the data. Sand P is very coarse (Geldart[20] class D) and shows no consolidation; the prefluidization flow breaks up any compaction. Thus, the difference between values of U_m for increasing and decreasing flow is small.

The rest of this paper uses data from the decreasing flow experiments, as is conventional.

3.5. Effect of Bed Height (*H*). Figure 10 shows the effect of bed height on U_m. For both distributors with all holes open and with half the holes open, U_m increased slightly with H up to around $H = 0.15$ m and then fell gently with increasing H. The effect is at most a factor of 2 in U_m for a given sand and K_p.

However, when only a quarter of the distributor holes were open, H had no apparent effect for either distributor. This is coincident with the problem with leaks around the tape and the change in hole spacing. Visually the solids' movement is independent of distributor characteristic, so the solids' movement probably does not account for the lack of effect of H on U_m when a quarter of the distributor holes were open.

Figure 11 shows that the experimental data of Dusad[12] from a rectangular bed demonstrate a similar effect of H on U_m. The effect is greater for the distributor with lower pressure drop (648 holes rather than 338 holes). Both distributors were made by laser drilling to a high standard. The data in Figure 11 are the average of the three wind box arrangements, which were not found to have a significant systematic effect.

The increase and then fall in U_m with bed height cannot be accounted for by the traditional method of critical pressure drop ratio. The theory of Fakhimi and Harrison[2] does not predict any effect of H. The theory

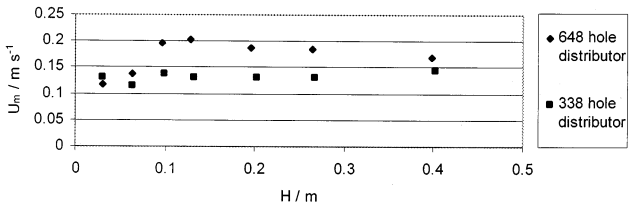

Figure 11. Effect of bed height (H) on U_m observed by Dusad[12] using a bed of cross section 0.1 m × 0.2 m.

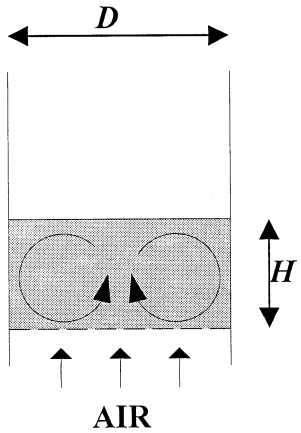

Figure 12. Proposed solids' circulation pattern, with $H \cong 0.5D$.

of Yue and Kolaczkowski[3] includes a term for H and is considered against our experimental data in section 5.2.

The observed effect of height may be due to the circulation of particles within the bed. Circulation patterns are particularly developed in large fluidized beds[6] often with an upward flow of solids near to the wall. However, we observed a downward flow of solids at the wall, the difference possibly due to the slugging character of our beds. Figure 12 postulates a circulation pattern which would be most significant when $H \sim 0.5D$. In our experiments, $0.5D = 145$ mm, which closely corresponds to the highest values of U_m in Figure 10.

Whitehead et al.[23] investigated particle circulation within large fluidized beds and found it to hinder good distribution and thus give higher U_m, as observed in our experiments. They observed a downward flow in the center and at the wall. Further experimental work is needed to establish the exact role of H. Circulation patterns could be investigated using particle tracking or imaging techniques.

4. Entry Zone

4.1. Background. The height of the entry zone (h) is an important parameter in the theory of Fakhimi and Harrison[2] (see Figure 3). The flow pattern above a distributor orifice is complicated, as illustrated by Figure 13, showing a jet above the orifice that forms bubbles a distance h above the distributor.

4.2. Two-Dimensional Beds. With two-dimensional fluidized beds, the entry zone can be observed visually and therefore more data are available in the literature for 2D than 3D beds.

Fakhimi and Harrison[2] suggest, for a two-dimensional bed, that $h = 3.8s$, eq 4. This result is based on experiments with superficial velocity, U, a little above U_{mf}, and it was observed that there was no significant effect upon h from U or orifice diameter, d_o.

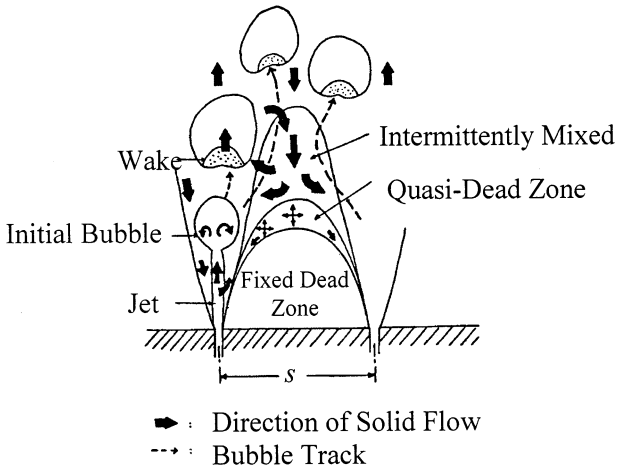

Figure 13. Region above the distributor plate (Compare Wen et al.[24]).

By using colored particles, Wen et al.[24] investigated the entry zone defined as the region where there was no particle mixing: h was found to depend on s and d_o but not H. No correlations were given for h, but at the lowest recorded U, the graphs indicate

$$h/s \sim 0.25 \tag{17}$$

h falls to zero at high U. There is a huge difference between eqs 17 and 4. This may be because Wen et al.[24] operated well above U_{mf}, or because they defined h as the height of the dead zone rather than the height of the jets (see Figure 13).

Yue and Kolaczkowski[3] report $h \propto q^{0.6}$, where q is the flow through each orifice; for a two-dimensional bed, $q = U \times s \times$ (width of bed), and combining these relations gives

$$h \propto U^{0.6} s^{0.6} \tag{18}$$

So h is predicted to increase with flow, contrary to the findings of Wen et al.[24] Note that eq 18 is not dimensionless, which implies that other parameters affect the jet length.

Thus, even for two-dimensional beds the literature is divided as to the effect of U on h. If either eq 18 or the results of Wen et al.[24] are used to eliminate $[h/s]$ in eq 3, the resulting equation is irrational and an iterative solution is required. Equation 4 is much simpler and is successfully used with eq 3 in section 5.1 to predict U_m.

4.3. Literature Review: Three-Dimensional Beds. Three-dimensional beds are of principal interest because of their use in industry: the difficulty is that the flow pattern within the bed cannot be observed visually. The correct relation between h and s has, therefore, to be inferred indirectly.

Lewin[18] and Taylor[19] followed the experimental finding of Rooney,[5] eq 5, ($h = 2s$) when applying the theory of Fakhimi and Harrison[2] to three-dimensional multi-orifice distributors. However, Rooney's data show h/s varying from 1.1 to 2.9 with an average value of 2. Also, the smallest orifice spacing investigated by Rooney was 18.1 mm; in our experiments s varied from 5 to 10 mm. Thus, there is some uncertainty in the use of the theory of Fakhimi and Harrison with eq 5, due to uncertainty about the height of the entry zone, h.

Rooney observed some effect of particle diameter, but no effect of U, contrary to the results of other authors, although her experiments covered a fairly small range of U ($U < 2U_{mf}$).

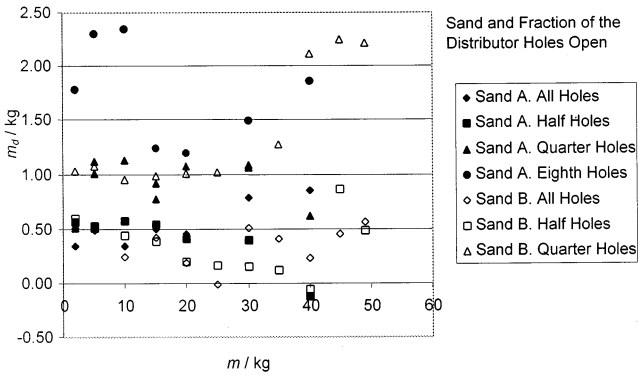

Figure 14. Graph to show the mass of sand that is not fluidized (m_d).

Fakhimi et al.[25] derived a theoretical equation to predict the height of the entry zone in a three-dimensional bed. Their equation showed h diminishing as U increased, but the equation matched experiments only when $U > 3U_{mf}$; so in preference, we used eq 5 with eq 3 to predict U_m (section 5.1). Nothing better than eq 5 could be found from the literature.

4.4. Experimental Investigation of *h*. Figure 8 shows that the bed pressure drop (ΔP_b) is slightly lower than the theoretical pressure drop required to support the bed (ΔP_t), even when the bed was evenly fluidized. Let the difference in pressure drops (ΔP_w) be defined as

$$\Delta P_w = \Delta P_t - \Delta P_b \tag{19}$$

Nonzero values of ΔP_w were noted by Whitehead and Dent[4] but not explained. ΔP_w can be interpreted as being due to the mass of sand, m_d, resting on the distributor plate and therefore not fluidized: thus, $\Delta P_w A = m_d g$ and, with eq 19,

$$m_d = m - \frac{\Delta P_b A}{g} \tag{20}$$

where m is the mass of sand in the bed. Using the hypothesis that, in the entry zone, ΔP_w is caused by defluidized sand resting on the distributor between the orifices and assuming that the geometry of the entry zone remains similar for different orifice spacings, then we speculate that

$$h \propto m_d \tag{21}$$

see section 4.6 below.

Values of m_d were estimated using eq 20, with data from experiments when the bed was evenly fluidized. The resulting average values of m_d are plotted in Figure 14, which shows the mean m_d plotted against m for different values of s (i.e. hole spacing). It is expected that m_d should not depend on m.

Figure 14 shows much scatter. But eq 20 involves taking the difference between two experimental measurements of nearly the same value, giving the well-known effect of amplifying percentage errors. Thus, the value of m_d is sensitive to m and ΔP_b, which is itself sensitive to the pressure in the windbox, $P_{wb,g}$, K_p (which has some uncertainty, see section 3.1), and the assumption that ΔP_d is unaffected by introducing the sand bed. Much of the scatter in Figure 14 is caused by random

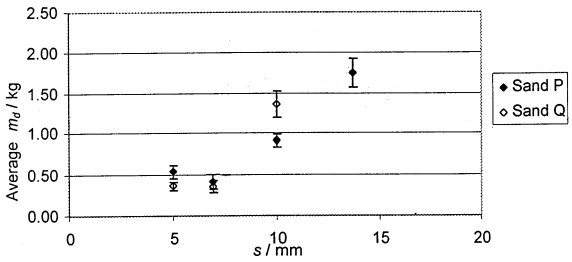

Figure 15. Graph to show the mean mass of sand that is not fluidized, m_d, determined from eq 20.

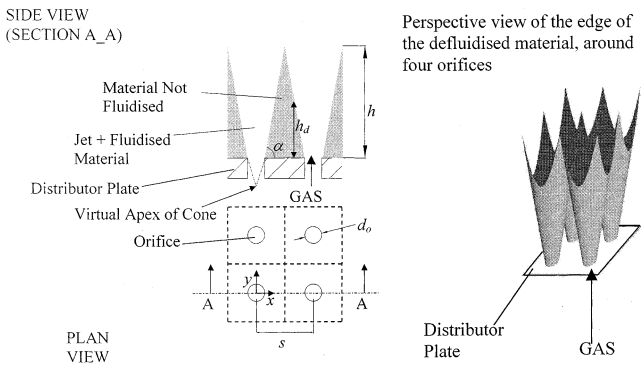

Figure 16. Theoretical model of the entry zone.

experimental error, but this cannot entirely account for all of it. In the next section we show that m_d depends on s, an expectation confirmed by Figure 15.

Figure 15 shows that m_d (and thus h) increases roughly linearly with s. An approximate correlation is $m_d/\text{kg} = 0.1s/\text{mm}$. This cannot be converted to a correlation for the height of the entry zone, h, without a geometric model of the entry zone, which is developed in the next section. Nonetheless, Figure 15 does verify the trend $h \propto s$ from our preferred correlation for h, eq 5.

4.5. Theoretical Model of the Entry Zone. Figure 16 shows a model of the entry zone in which inverted cones of air and fluidized material are formed above each orifice.

Between the orifices and cones is sand, not fluidized, resting on the distributor plate. The cones meet at the top of the entry zone, thus defining h. At a given position (x,y) on the distributor plate, see Figure 16, the height of sand above the plate, h_d, is given by $h_d = ((x^2 + y^2)^{0.5} - {}^1/_2 d_o)\tan\alpha$. α is the cone angle related to h/s; thus, for $h/s = 2$, $\alpha \sim 76°$. The mass of sand per orifice m_d/N is obtained by performing a volume integration over the region surrounding the orifice, giving

$$\frac{m_d}{N} = \left(\int_{-s/2}^{s/2}\int_{-s/2}^{s/2} h_d \, dy \, dx + \frac{\pi d_o^3}{24}\tan\alpha\right)\rho_s(1-\epsilon_{mf}) \quad (22)$$

Note that the term $(\pi d_o^3 \tan\alpha)/24$ is to correct for the negative values of h_d within the area of the orifice; that is, this term discounts the material in the cone that is beneath the level of the top of the distributor plate, shown dotted and dashed in Figure 16.

On substitution for h_d, eq 22 can be solved analytically (as was pointed out by one of the reviewers), but the answer is long-winded. Since we require numerical answers for m_d, it is easier to integrate numerically. The following answer has been obtained by three independent methods, the first supplied by the aforementioned reviewer.

Table 7. Theoretical m_d Values Based on Eq 23 Compared with the Experimental Correlation for m_d Derived from Figure 15

distributor holes open	s^a/mm	theor m_d/kg	correlation 0.1s/kg
all holes	5	0.45	0.5
half of holes	7.1	0.75	0.71
quarter of holes	10	1.17	1.0
eighth of holes	14.1	1.76	1.41

[a] The values of s for the half holes and eighth holes are average separations and are based on s^2N = constant = $5^2 \times 2561$ mm^2. This approach was suggested by the aforementioned reviewer.

$$\frac{m_d}{N} = \left(0.3826s^3 - \frac{d_o s^2}{2} + \frac{\pi d_o^3}{24}\right)(\tan\alpha)\rho_s(1-\epsilon_{mf}) \quad (23)$$

The theoretical values for m_d based on eq 23 are reported in Table 7, for $d_o = 1.5$ mm (distributor A), $\alpha = 76°$, and N which is reported in Figure 7.

Figure 15 suggests that our experimental values of m_d are adequately correlated by 0.1s, and results from this correlation are also given in Table 7. There is little difference between the correlation and the theoretical values. The theory therefore agrees quite well with the experimental values shown in Figure 15.

4.6. Comparison of Experimental and Theoretical m_d. The theoretical value of m_d depends on α, but α is uncertain. For orifices with vertical axes, the defluidized material is stabilized by the jetting action and pressure of the gas as it passes through the orifices; as a result, α will have a value greater than the free angle of repose, about 35° for sand. α is probably greater than the angle of the stagnant zone boundary in a silo, about 45° for sand. From Table 7 it seems that a value of 76° for α, which corresponds well with the relation $h = 2s$, eq 5, is representative of the multiorifice distributors used in our experiments. For tuyere distributors, like those of Whitehead and Dent,[4] α is likely to be much less than 76° because the horizontal jets will undermine the heaps of defluidized material. The relation $h = 0.5s$, eq 6, implies a value of α of 45°, which is plausible.

The above is all consistent with the hypothesis outlined above that the small deficit in pressure drop across fluidized beds is caused by defluidized material resting on the distributor plate.

5. Evaluation of Theoretical Predictions of Maldistribution

5.1. Fakhimi and Harrison.[2] Predictions of U_m from the theory of Fakhimi and Harrison, eq 3, are compared to experimental values of U_m from this project and from the literature (see Table 2 for details of the complete experimental data set) by calculating the ratio of experimental U_m to theoretical U_m. In calculating the theoretical values, the relation $h = 2s$ was used for multiorifice distributors and the relation $h = 0.5s'$ was used for the data of Whitehead and Dent,[4] where tuyeres were used. The results are shown in Figure 17. The average error in the predicted U_m is 18%, and virtually all of the theoretical predictions of U_m lie within a factor of 2 of the experimental values, a large improvement over the traditional pressure drop ratio method (Figure 2).

If the data set of Whitehead and Dent[4] is considered on its own, the average error in U_m, as predicted by the

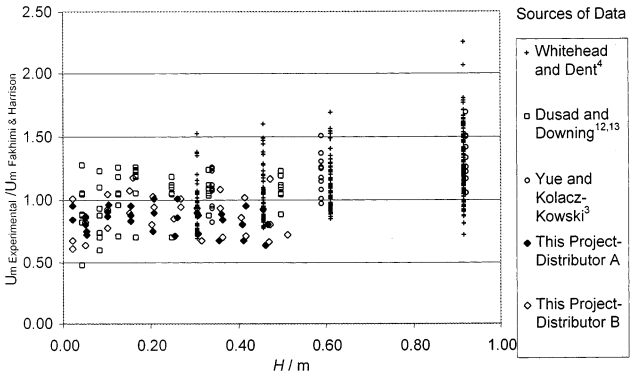

Figure 17. Ratio (experimental value of U_m)/(prediction of Fakhimi and Harrison,[2] eq 3) plotted against the height of the bed, H, which should have no effect.

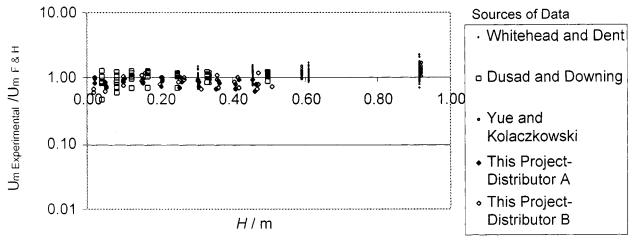

Figure 18. Graph to show the effectiveness of the prediction of U_m, eq 3, based on the work of Fakhimi and Harrison.[2] Compare Figure 2.

theory of Fakhimi and Harrison,[2] is also 18%. This compares acceptably to the 10% average error claimed by Whitehead and Dent[4] for their own formula. Part of the extra error may be due to using eq 6 to predict h for the two different designs of tuyere of Whitehead and Dent,[4] which had the gas exits at different heights above the distributor plate. Bed height (H) is not a factor in the Fakhimi and Harrison[2] analysis. Figure 17 shows that the assumption that H is unimportant is nearly valid, although our experimental data (Figure 10) and data from Dusad[12] (Figure 11) do reveal some effect.

The data from Figure 17 are replotted in semilogarithmic fashion in Figure 18 so that the effectiveness of the theory of Fakhimi and Harrison,[2] eq 3, can be compared visually to the results from the critical pressure drop ratio method[1] shown in Figure 2. It is clear that the match between experiment and theory appears much better when the theory of Fakhimi and Harrison[2] is used to predict maldistribution.

This observation is true, notwithstanding the use of a ratio of U_m values in Figure 18 instead of R, the ratio of ΔP values. The reader is reminded that $U^2 \propto \Delta P_d$, and this means that deviations in log R from any baseline are amplified by a factor of 2 compared to a ratio of velocities. The maximum deviation in R about the best value of R ($\cong$0.1) in Figure 2 is a factor of 33. The maximum deviation in Figures 17 and 18 is a factor of 2. For direct comparability, the factor of 33 should be reduced to its square root, which is a factor of 6. Thus, in terms of U_m, the method based on the theory of Fakhimi and Harrison appears to be about three times superior to the traditional method.[1] In terms of distributor pressure drop, it is nine times superior.

5.2. Yue and Kolaczkowski.[3] This theory is discussed in section 1.3 and gives rise to eq 14: it has an extra $\epsilon_b H_{mf}$ term compared with the theory of Fakhimi and Harrison,[2] eq 3. The effect of the extra term is to increase U_m above the Fakhimi and Harrison[2] predictions for tall fluidized beds and for those operated well in excess of U_{mf} (as these have high ϵ_b). Figure 17 shows that the data of both Whitehead and Dent[4] and Yue and Kolaczkowski[3] show slightly higher U_m when compared to the theory of Fakhimi and Harrison[2] for taller beds. However, the scatter in the data is larger than this effect.

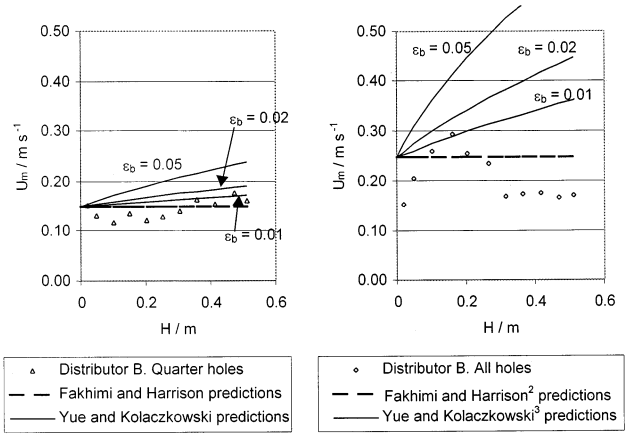

Figure 19. (A (left) and B (right)) Graphs testing Yue and Kolaczkowski's[3] predictions against experimental data from this project. See Table 3 and Figure 7 for distributor details.

The theory of Yue and Kolaczkowski[3] relies on the bubble fraction (ϵ_b) in the bed. Correlations are suggested, but these are complicated, and an iterative procedure is required. We made experimental measurements of H when the bed was evenly fluidized and estimated $\epsilon_b = 0.01-0.05$. Yue and Kolaczkowski[3] worked on 2D beds and suggest ϵ_b is typically 0.1−0.2. In our experiments U_m is fairly close to U_{mf}, which should give a lower ϵ_b. Figure 19 presents some of our experimental data for 3D beds and the Yue and Kolaczkowski[3] predictions with a range of ϵ_b. The theory predicts U_m to increase with bed height (H), but this does not match our experimental trends (U_m increases and then decreases with H or is fairly independent of H.)

The theory is not tested against the other experimental data because of the difficulty of determining ϵ_b. However, the effect of height on the prediction of U_m by Fakhimi and Harrison[2] (Figure 19) is far smaller than that predicted by Yue and Kolaczkowski[3] for a reasonable ϵ_b.

Figure 19 suggests that the agreement of the predictions of Yue and Kolaczkowski[3] with experiment is poorer than that of the simpler theory of Fakhimi and Harrison,[2] which we therefore favor.

5.3. General Comparison. Although the fit between the theory of Fakhimi and Harrison[2] and experimental data (Figure 17) is good, there are some areas of uncertainty. Bed height (H) had an effect on U_m for distributors with more holes. This could be caused by entry effects, but literature suggests that the entry zone effects are independent of bed height. Another hypothesis is that the effect of height is caused by circulation within the bed. Further theoretical analyses are probably more useful than correlations of the data, which tend to become inapplicable outside of the initial data set, particularly as there is a large scatter in the reported U_m values. Further experiments and a closer analysis of the data from Whitehead and Dent[4] could show whether the trends of U_m with H seen in this work (Figure 10) and by Dusad[12] and Downing[13] (Figure 11)

are confirmed. In addition, circulation within the bed may be important.

The height of the entry zone (h) is the other area of uncertainty. There is more information in the literature on this subject, though conflicting. Experiments to study flow regimes near distributors would be possible, for example by putting pressure or capacitance probes in the bed or through the distributor plate[5] or by using X-ray or other tomographic techniques

6. Conclusions

Published experimental data on the limiting velocity for maldistribution in bubbling fluidized beds, U_m, were assembled. The data were measured in a variety of sizes and shapes of bed and for a variety of granular materials in Geldart[20] groups B and D; there were two main distributor types, multiorifice and tuyere. These data were added to experimental results reported in this paper. The resulting large data set was used to evaluate published methods of predicting the onset of maldistribution.

The theory of Fakimi and Harrison,[2] eq 3, when combined with reliable predictions for h, eqs 4−6, was found to predict the transition velocity, U_m, between even fluidization and maldistribution within a factor of 2, much better than the critical pressure drop ratio method[1] in common use that showed errors in excess of a factor of 6 for the assembled data set. Fakimi and Harrison's theory is based on the hypothesis that maldistibution is due to an entrance effect at the distributor, similar for multiorifice and tuyere distributors. It is therefore not suprising that it is effective in describing the behavior of both kinds of distributor.

The theory of Yue and Kolaczkowski[3] attempts to improve on that of Fakhimi and Harrison by including an effect of bed height. Yue and Kolaczkowski found support for their theory in their own experiments with a two-dimensional fluidized bed. When their theory was tested against our data set, it was found to be no better than the simpler theory of Fakhimi and Harrison.

7. Nomenclature

A = area of bed (m^2)
a_o = area of an orifice (m^2)
c_d = orifice discharge coefficient (−)
D = bed diameter (m)
D_s = depth of material in fluidized bed at minimum fluidization (ft) = H_{mf}
d_o = orifice diameter (m)
d_p = particle diameter (m)
g = acceleration due to gravity ($m \cdot s^{-2}$)
H = bed height (m)
H_{mf} = bed height at minimum fluidization (m)
h = height of entry zone (m)
h_d = height of sand that is not fluidized (m)
k = constant in the equation developed by Whitehead and Dent[4] (in $wg \cdot ft^2/(3600\ lb)$)
k' = constant in eq 8 ($m \cdot s^{-2}$)
K_D = Whitehead and Dent[4] distributor characteristic (60 $ft/(s\ (in\ wg)^{0.5})$)
K_p = distributor characteristic ($=\Delta P_d/\rho_g U^2$) (−)
m = mass of sand in the bed (kg)
m_d = mass of sand that is not fluidized (kg)
N = number of orifices (−)
n = number of active holes (−)
$P_{wb,g}$ = windbox pressure (Pa, gauge)
q = orifice flow ($m^3\ s^{-1}$)
q_1 = bubbling orifice flow ($m^3 \cdot s^{-1}$)
q_{mf} = orifice flow at incipient fluidization ($m^3 \cdot s^{-1}$)
R = pressure drop ratio ($=\Delta P_d/\Delta P_b$) (−)
s = orifice spacing (m)
s' = modified tuyere spacing = tuyere center to center spacing − tuyere diameter (m)
t = plate thickness (m)
U = superficial velocity ($m \cdot s^{-1}$)
U_1, U_2 = superficial velocity in sections 1 and 2 of the bed as shown in Figure 5 ($m \cdot s^{-1}$)
U_m = superficial velocity at onset of even fluidization ($m \cdot s^{-1}$)
V_o = jet velocity ($m \cdot s^{-1}$)
x,y = coordinates in Figure 16 (m)
α = angle of piles of sand
δ = small number
δq = change in flow ($m^3 \cdot s^{-1}$)
ΔP = pressure drop (Pa)
ΔP_b = bed pressure drop (Pa)
$\Delta P_{b,mf}$ = bed pressure drop at incipient fluidization (Pa)
$\Delta P_{b1,2}$ = bed pressure drop in region 1 or 2 (Pa)
ΔP_d = distributor pressure drop (Pa)
$\Delta P'_d$ = distributor pressure drop ($kg \cdot m^{-2}$)
$\Delta P_{d1,2}$ = distributor pressure drop at incipient fluidization (Pa)
$\Delta P_{d,mf}$ = distributor pressure drop at incipient fluidization (Pa)
$\Delta P_{d,min}$ = minimum distributor pressure drop (Pa)
$\Delta P_{ez,mf}$ = pressure drop over the entry zone at incipient fluidization (Pa)
ΔP_s = pressure drop across a jet (Pa)
ΔP_t = theoretical bed pressure drop to support the weight of the bed (Pa)
ΔP_w = cifference between the pressure drop to support the weight of the bed and the actual bed pressure drop ($\Delta P_w = \Delta P_t - \Delta P_b$) (Pa)
ϵ_{mf} = voidage fraction in particulate phase at incipient fluidization (−)
ϵ_b = bubble volume fraction (−)
ρ_g = gas density ($kg \cdot m^{-3}$)
ρ_s = solid density ($kg \cdot m^{-3}$)

Appendix 1: Data from Yue and Kolaczkowski[3]

Yue and Kolaczkowski[3] present experimental data from their two-dimensional rig. They report U_m, h, and s, but not U_{mf}, so this was estimated using the Ergun equation. K_p was obtained from a graph of ΔP_d against gas jet velocity through the orifices (V_o), using

$$K_p = \left(\frac{\Delta P'^{1/2}_d}{V_o}\right)^2 \frac{gA^2}{\rho_g a_o^2 N^2} \qquad (24)$$

where $\Delta P'_d$ is measured in $kg \cdot m^{-2}$. The graph of $[\Delta P'_d]^{1/2}$ against V_o given by Yue and Kolaczkowski[3] had the V_o axis labeled as "$V_o \times 10^2$ ($m \cdot s^{-1}$)", which corresponds to a maximum jet velocity of 0.8 $m \cdot s^{-1}$, which is unreasonably small. The corresponding K_p was small and $c_d \gg 1$, which is also unreasonable. It was therefore assumed that the axis should have been labeled "V_o ($m \cdot s^{-1}$)", corresponding to a more reasonable maximum jet velocity of 80 $m \cdot s^{-1}$. This gives K_p as 97 600 and c_d of 0.64, which is reasonable. Note that all of Yue and Kolaczkowski's data[3] had the same K_p.

Literature Cited

(1) Perry, R. H., Green, D. W., Maloney, J. O., Eds. *Perry's Chemical Engineers' Handbook*, 7th ed.; McGraw-Hill: New York, 1997; p 17-6.

(2) Fakhimi, S.; Harrison, D. Multi-Orifice Distributors in Fluidised Beds: A Guide to Design. In *Chemeca '70*; Butterworth: Australia, 1970; p 29.

(3) Yue, P. L.; Kolaczkowski, J. A. Multiorifice Distributor Design for Fluidised Beds. *Trans. Inst. Chem. Eng.* **1982**, *60*.

(4) Whitehead, A. B.; Dent, D. C. Behaviour of multiple tuyere assemblies in large fluidised beds. In *Proceedings of the International Symposium on Fluidisation*, Eindhoven, June 6−9; Drinkenburg, A. A. H., Ed.; Netherlands University Press: Amsterdam, 1967; p 802.

(5) Rooney, N. M. Distributors and Obstacles in Fluidised Beds. Ph.D. Thesis, Department of Chemical Engineering, University of Cambridge, 1974.

(6) Geldart, D.; Bayerns, J. The design of distributors for gas fluidised beds. *Powder Technol.* **1985**, *42*, 67.

(7) Zenz, F. A.; Othmer, D. F. *Fluidization and Fluid Particle Systems*; Rheinhold: New York, 1960; p 260.

(8) Agarwal, J. C.; Davis, W. L.; King, D. T. *Chem. Eng. Prog.* **1962**, *58*, 85.

(9) Hiby, J. W. Untersuchungen über den Kritischen Mindestdruckverlust des Antrömbdens bei Fluidalbetten (Fleiessbetten). *Chem. Ing. Tech.* **1964**, *36*, 228.

(10) Avery, D. A.; Tracey, D. H. The application of fluidised beds of activated carbon. In *Proceedings of the I Chem E Symposium*, Montreal, Canada; I Chem E: London, 1968; p 28.

(11) Thorpe, R. B.; Davidson, J. F.; Downing, S. J.; Dusad, A.; Farthing, P.; Ferdinando, G.; Holden, A.; Martin, A.; Negyal, O.; Saundry, J. On the minimum distributor pressure drop for uniform fluidization. In *Proceedings of 3rd. European Conference on Fluidization*, Toulouse, 29−31 May 2000; SFGP: Nancy, France, p 189.

(12) Dusad, A. The study of Maldistribution in Fluidised Beds. Part II Project, Department of Chemical Engineering, University of Cambridge, 1999.

(13) Downing, S. J. The study of Maldistribution in Fluidised Beds. Part II Project, Department of Chemical Engineering, University of Cambridge, 1999.

(14) Qureshi, A. E.; Creasy, D. E. Fluidised bed gas distributors. *Powder Technol.* **1979**, *22*, 113.

(15) Sathiyamoorthy, D.; Sridar Rao, C. The choice of distributor to bed pressure-drop ratio in gas-fluidised beds. *Powder Technol.* **1981**, *30*, 139−143.

(16) Davidson, J. F.; Harrison, D.; Darton, R. C.; LaNauze, R. D. Two phase theory of fluidisation and its application to Chemical Reactors. In *Chemical Reactor Theory, A Review*; Lapidus, L., Amundson, N., Eds.; Prentice Hall Inc.: Upper Saddle River, NJ, 1977; p 583.

(17) Lefroy, G. A.; Davidson, J. F. The mechanics of spouted beds. *Trans. Inst. Chem. Eng.* **1969**, *47*, 120.

(18) Lewin, S. Maldistribution in Fluidised Beds. Part IIB Project, Department of Chemical Engineering, University of Cambridge, 2000.

(19) Taylor, A. L. Maldistribution in Fluidised Beds. Part IIB Project, Department of Chemical Engineering, University of Cambridge, 2000.

(20) Geldart, D. Types of Gas Fluidisation. *Powder Technol.* **1973**, *7*, 285.

(21) Farthing, P. Investigation into Maldistribution in Fluidised Beds. Part II Project, Department of Chemical Engineering, University of Cambridge, 1999.

(22) Ferdinando, G. Investigation into Maldistribution in Fluidised Beds. Part II Project, Department of Chemical Engineering, University of Cambridge, 1997.

(23) Whitehead, A. B.; Gartside, G.; Dent, D. C. Flow and Pressure Maldistribution at the Distributor Level of a Gas−solid Fluidised Bed. *Chem. Eng. J.* **1970**, *1*, 175.

(24) Wen, C. Y.; Krishnan, R.; Khosravi, R.; Dutta, S. Dead zone heights near the grid of fluidised beds. In *Proceedings of the 2nd Engineering Foundation Conference*, Cambridge, April 2−6; Davidson, J. F., Keairns, D. L., Eds.; Cambridge University Press: Cambridge, 1978; p 32.

(25) Fakhimi, S.; Sohrabi, S.; Harrison, D. Entrance effects at a multiorifice distributor in gas fluidised beds. *Can. J. Chem. Eng.* **1983**, *61*, 364.

(26) Pollitt, M. Maldistribution in fluidised beds. Part IIB Project, Department of Chemical Engineering, University of Cambridge, 2001.

Received for review April 29, 2002
Revised manuscript received August 14, 2002
Accepted August 14, 2002

IE0203173